Computers in Biology and Medicine 87 (2017) 371–381

Contents lists available at ScienceDirect

Computers in Biology and Medicine

journal homepage: www.elsevier.com/locate/compbiomed

Computing dispersion curves of elastic/viscoelastic transversely-isotropic bone plates coupled with soft tissue and marrow using semi-analytical finite element (SAFE) method

Vu-Hieu Nguyen [a], Tho N.H.T. Tran [b], Mauricio D. Sacchi [c], Salah Naili [a], Lawrence H. Le [b,c,*]

[a] Laboratoire Modélisation et Simulation Multi Echelle UMR 8208 CNRS, Université Paris-Est, Créteil, France
[b] Department of Radiology and Diagnostic Imaging, University of Alberta, Edmonton, Alberta T6G 2B7, Canada
[c] Department of Physics, University of Alberta, Edmonton, Alberta T6G 2G7, Canada

ARTICLE INFO

Keywords:
Ultrasound
Semi-analytical finite element (SAFE)
Cortical bone
Axial transmission
Guided waves
Phase velocity
Group velocity
Energy velocity
Dispersion
Attenuation
Transverse isotropy

ABSTRACT

We present a semi-analytical finite element (SAFE) scheme for accurately computing the velocity dispersion and attenuation in a trilayered system consisting of a transversely-isotropic (TI) cortical bone plate sandwiched between the soft tissue and marrow layers. The soft tissue and marrow are mimicked by two fluid layers of finite thickness. A Kelvin-Voigt model accounts for the absorption of all three biological domains. The simulated dispersion curves are validated by the results from the commercial software DISPERSE and published literature. Finally, the algorithm is applied to a viscoelastic trilayered TI bone model to interpret the guided modes of an *ex-vivo* experimental data set from a bone phantom.

1. Introduction

Cortical bone supports most of the mechanical load of the body and bone quality is affected by aging and osteoporosis. The bone disease causes loss of bone mass and deterioration of bone micro-architectures, leading to fracture risks. Developing effective diagnostic techniques to prevent osteoporotic fractures has attracted worldwide efforts to save lives. Among all methods, quantitative ultrasound (QUS) has demonstrated its promising potential in the *in-vivo* assessment of bone integrity [1]. An advantage of QUS over the gold-standard dual X-ray absorptiometry (DXA) is its ability to provide the mechanical properties, relevant to bone quality. Moreover, ultrasound is non-ionizing and the ultrasonic apparatus is relatively inexpensive in comparison with X-ray devices.

Axial transmission (AT) technique has been developed [2] to study cortical long bones *ex vivo* and *in vivo*. The AT acquisition uses a set of ultrasonic transducers (transmitter and receiver) placed collinearly in contact with the bone or skin and approximately parallel to the bone's longitudinal direction. The transmitter emits ultrasound pulses and the receiver records the signals after their propagation along the cortex. Transducer arrays [3,4] have been used to speed up the acquisition process. Nguyen et al. [3] grouped several elements as source to increase transmitting energy and steer the ultrasound beam for guided mode selectivity. Minonzio et al. [4] used a transducer array to generate a multi-emitter/multi-receiver data set for dedicated signal processing. Non-contact technique such as photo-acoustic excitation and optical detection was also developed to study ultrasonic guided waves in bone phantoms [5].

The assessment of the geometrical and mechanical properties of the cortical bone is based on detecting the time of flight of first arriving signals [6–8] or identifying specific modes of guided waves [9–12] propagating along the long bone. For modeling purposes, the cortical bone is usually described as plate-like [6–8,13,14] or cylindrical-like waveguides [12,15,16]. Our understanding of coupling effects due to the presence of soft tissue and marrow layers on the characteristics of the guided modes is very limited. Moreover, absorption is usually neglected. The influence of the coupled soft medium and marrow on ultrasound waves in bones remains challenging due to the lack of computational methods that are able to accurately describe the dispersion phenomena of waves in a coupled fluid/solid/fluid system.

A few computational methods have been established for different

* Corresponding author. Department of Radiology and Diagnostic Imaging, University of Alberta, Edmonton, Alberta T6G 2B7, Canada.
E-mail address: lawrence.le@ualberta.ca (L.H. Le).

http://dx.doi.org/10.1016/j.compbiomed.2017.06.001
Received 12 April 2017; Received in revised form 31 May 2017; Accepted 2 June 2017

model structures. They are, for instance, the analytical method for orthotropic elastic plates immersed in fluid [17,18], the transfer matrix method for multilayered elastic media [19], the asymptotic method for functionally graded plates [16,20], and the spectral collocation method for generally anisotropic viscoelastic media in flat and cylindrical geometry [21]. Commercial tools such as DISPERSE (Imperial College London, UK) have also been developed. Recently, much attention has been devoted to the SAFE method due to its flexibility to handle complex geometries and multiphysics problems [22–25]. The SAFE method has also been demonstrated to simulate transient waves efficiently [26–30].

The aim of this work is to develop a SAFE formulation for computing the dispersion curves of a two-dimensional (2D) trilayered medium consisting of a viscoelastic and TI plate between two finite-thickness layers of viscous fluids. In Section 2, the momentum equations, boundary conditions, and the SAFE formulation of the characteristic equations are derived. The bone models used in this study are described in Section 3. Results related to validation and an application to interpret an *ex-vivo* data set are presented in Section 4. This will be followed by discussion and conclusion in Sections 5 and 6 respectively.

2. Formulation of the problem

2.1. Geometry of the model

A solid layer, extending infinitely along the $\mathbf{x}_1$ direction (Fig. 1), represents the cortical bone plate with a constant thickness h (domain $\Omega^b = \{(x_1, x_2); -h \le x_2 \le 0\}$). The anisotropic bone plate is sandwiched between the overlying soft tissue and the underlying marrow layer. Their respective domains are denoted by Ω_1^f ($\Omega_1^f = \{(x_1, x_2); 0 \le x_2 \le h_1\}$) and Ω_2^f ($\Omega_2^f = \{(x_1, x_2); -(h+h_2) \le x_2 \le -h\}$), where h_1 and h_2 are the thicknesses of the soft tissue and marrow layers respectively. The plane interfaces between the bone (Ω^b) and the fluids (Ω_1^f and Ω_2^f) are denoted by Γ_1^{bf} and Γ_2^{bf} respectively.

2.2. Governing equations and boundary conditions

Both soft tissue and marrow layers are modeled as acoustic fluid media with dissipation. The dissipation mechanism is assumed to be small and due only to viscosity without memory effects [8,31]. The linearized wave equations of wave propagation in both domains Ω_1^f and Ω_2^f are

$$\rho_\alpha \ddot{p}_\alpha - K_\alpha \nabla^2 (p_\alpha + \gamma_\alpha \dot{p}_\alpha) = 0, \quad \forall \mathbf{x} \in \Omega_\alpha^f, (\alpha = 1, 2) \tag{1}$$

where p_α ($\alpha = 1, 2$) denotes the acoustic pressure in Ω_α^f; K_α and ρ_α are the bulk modulus at rest and the mass density of the fluid, respectively; γ_α denotes the viscosity coefficient; single dotted and double dotted symbols indicate the first and second order time derivatives respectively. Thus the wave velocity in Ω_α^f is $c_\alpha = \sqrt{K_\alpha/\rho_\alpha}$.

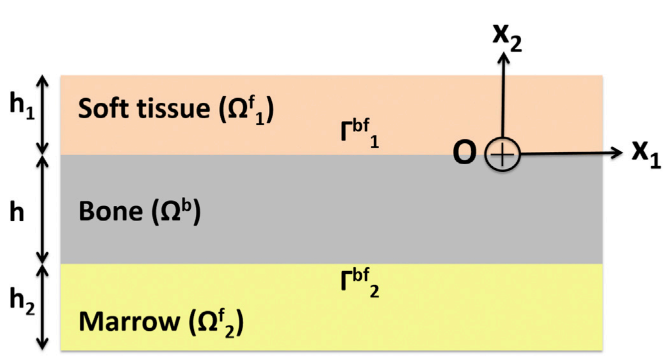

Fig. 1. Geometry of the trilayered bone model.

In Ω^b, the displacement vector is denoted by $\mathbf{u}(\mathbf{x}, t) = \{u_1, u_2\}^T$ while the stress and strain vectors are $\boldsymbol{\sigma} = \{\sigma_{11}, \sigma_{22}, \sigma_{12}\}^T$ and $\boldsymbol{\varepsilon} = \{\varepsilon_{11}, \varepsilon_{22}, 2\varepsilon_{12}\}^T$ respectively. Then the dynamic equilibrium equation is

$$\rho \ \ddot{\mathbf{u}} - \mathbb{L}^T \boldsymbol{\sigma} = \mathbf{0} \tag{2}$$

where ρ is the mass density and the operator $\mathbb{L}$ is defined by

$$\mathbb{L} = \mathbf{L}_1 \partial_1 + \mathbf{L}_2 \partial_2, \quad \mathbf{L}_1 = \begin{bmatrix} 1 & 0 \\ 0 & 0 \\ 0 & 1 \end{bmatrix}, \quad \mathbf{L}_2 = \begin{bmatrix} 0 & 0 \\ 0 & 1 \\ 1 & 0 \end{bmatrix} \tag{3}$$

with ∂_1 and ∂_2 being the spatial derivatives along the $\mathbf{x}_1$ and $\mathbf{x}_2$ directions respectively.

The constitutive law describing the Kelvin-Voigt viscoelastic behavior of the bone is

$$\boldsymbol{\sigma} = \mathbf{C}\boldsymbol{\varepsilon} + \boldsymbol{\eta}\dot{\boldsymbol{\varepsilon}}, \quad \boldsymbol{\varepsilon} = \mathbb{L}\mathbf{u}, \tag{4}$$

where $\mathbf{C}$ and $\boldsymbol{\eta}$ are the elasticity and viscosity tensors respectively [28]. We recall that the material properties of the trilayered system depend only on $\mathbf{x}_2$, i.e. $\rho = \rho\,(x_2)$, $\mathbf{C} = \mathbf{C}\,(x_2)$ and $\boldsymbol{\eta} = \boldsymbol{\eta}\,(x_2)$.

Regarding the boundary conditions, the normal velocity and stresses are continuous at the fluid-solid interfaces, i.e.

$$\left.\begin{array}{l} \partial_2 \left(p_\alpha + \gamma_\alpha \dot{p}_\alpha\right) = -\rho_\alpha \ddot{u}_2, \\ \{\sigma_{12}, \sigma_{22}\}^T = \{0, -(p_\alpha + \gamma_\alpha \dot{p}_\alpha)\}^T, \end{array}\right\} \quad \forall \mathbf{x} \in \Gamma_\alpha^{bf} \quad (\alpha = 1, 2) \tag{5}$$

where $\{\sigma_{12}, \sigma_{22}\}^T$ is the traction. The free boundary conditions for fluid layers are

$$p_\alpha = 0, \quad \forall\, \mathbf{x} \in \Gamma_\alpha^f \quad (\alpha = 1, 2) \tag{6}$$

2.3. Corresponding equations in the frequency-wavenumber (ω-k) domain

We look for solutions of harmonic waves propagating along the axial direction $\mathbf{x}_1$ in the following form

$$p_\alpha(x_1, x_2, t) = \tilde{p}_\alpha(x_2) e^{i(k_1 x_1 - \omega t)}, \tag{7}$$

$$\mathbf{u}(x_1, x_2, t) = \tilde{\mathbf{u}}(x_2) e^{i(k_1 x_1 - \omega t)}, \tag{8}$$

where $i^2 = -1$, ω is the angular frequency, and k_1 denotes wavenumber in $\mathbf{x}_1$ direction. $\tilde{p}_\alpha(x_2)$ and $\tilde{\mathbf{u}} = (\tilde{u}_1, \tilde{u}_2)^T$ represent the amplitudes of pressure and displacement vector in the fluid and solid respectively. By substituting Eq. (7) into Eq. (1), the equations in the fluid layers become

$$\left(-\rho_\alpha \omega^2 + k_1^2 \overline{K}_\alpha\right) \tilde{p}_\alpha - \overline{K}_\alpha \partial_2^2 \tilde{p}_\alpha = 0, \quad \forall \mathbf{x} \in \Omega_\alpha^f, (\alpha = 1, 2) \tag{9}$$

where $\overline{K}_\alpha = K_\alpha (1 - i\omega\gamma_\alpha)$. Similarly, substituting Eq. (8) into Eq. (2) leads to

$$-\rho\omega^2 \tilde{\mathbf{u}} - \tilde{\mathbb{L}}^T \tilde{\boldsymbol{\sigma}} = \mathbf{0} \tag{10}$$

where $\tilde{\mathbb{L}} = ik_1 \mathbf{L}_1 + \mathbf{L}_2\, \partial_2$.

The corresponding constitutive law is

$$\tilde{\boldsymbol{\sigma}} = ik_1 \overline{\mathbf{C}} \mathbf{L}_1 \tilde{\mathbf{u}} + \overline{\mathbf{C}} \mathbf{L}_2 \partial_2 \tilde{\mathbf{u}}. \tag{11}$$

where $\overline{\mathbf{C}} = \mathbf{C} - i\omega\boldsymbol{\eta}$. The interface conditions are

$$\partial_2 \tilde{p} = \overline{\rho}_\alpha \omega^2 \tilde{u}_2, \quad \{\tilde{\sigma}_{12}, \tilde{\sigma}_{22}\}^T = \{0, -(1 - i\omega\gamma_\alpha)\tilde{p}_\alpha\}^T \tag{12}$$

where $\overline{\rho}_\alpha = \rho_\alpha / (1 - i\omega\gamma_\alpha)$. For each values of (ω, k_1), Eq. (10) can be rewritten as